Hyperfine Interact (2019) 240:66
https://doi.org/10.1007/s10751-019-1608-5

Hyperfine structure and nuclear magnetic moments of the praseodymium isotopes ^{135,136,137}Pr

Nadja Frömmgen[1] · Wilfried Nörtershäuser[1,2] · Mark L. Bissell[3,4] · Klaus Blaum[5] · Christopher Geppert[1,2] · Michael Hammen[1] · Magdalena Kowalska[6] · Jörg Krämer[1] · Kim Kreim[5] · Andreas Krieger[1,2] · Yuri A. Litvinov[7] · Rainer Neugart[1,5] · Gerda Neyens[3] · Jasna Papuga[3] · Rodolfo Sánchez[7] · Deyan T. Yordanov[5,8]

Published online: 12 June 2019

Abstract
Collinear laser spectroscopy was applied to measure the hyperfine structure of $^{135-137}$Pr at ISOLDE/CERN. Combined with measurements of the stable isotope ^{141}Pr at the TRIGA-SPEC setup in Mainz we were able to determine the magnetic moments of the neutron-deficient isotopes ^{135}Pr, ^{136}Pr and ^{137}Pr for the first time.

Keywords Hyperfine structure · Laser spectroscopy · Magnetic moments · Electron capture decay · Collinear laser spectroscopy · Praseodymium

1 Motivation

Properties of nuclear decays caused by the weak interaction can differ significantly for nuclei in highly charged ions compared to those embedded in the corresponding neutral atom [1, 2]. The isotope ^{140}Pr ($Z = 59$) decays to ^{140}Ce via an allowed Gamow-Teller decay ($\Delta\ell = 1$, no parity change) [3]. Thereby a proton is converted into a neutron either

This article is part of the Topical Collection on *Proceedings of the International Conference on Hyperfine Interactions and their Applications (HYPERFINE 2019), Goa, India, 10-15 February 2019* Edited by S. N. Mishra, P. L. Paulose and R. Palit

✉ Wilfried Nörtershäuser
wnoertershaeuser@ikp.tu-darmstadt.de

1 Institut für Kernchemie, Universität Mainz, D-55099 Mainz, Germany

2 Institut für Kernphysik, Technische Universität Darmstadt, D-64289 Darmstadt, Germany

3 Instituut voor Kern- en Stralingsfysica, KU Leuven, B-3001 Leuven, Belgium

4 Present address: School of Physics and Astronomy, The University of Manchester, Manchester M13 9PL, UK

5 Max-Planck-Institut für Kernphysik, D-69117 Heidelberg, Germany

6 Experimental Physics Department, CERN, CH-1211 Geneva, Switzerland

7 GSI Helmholtzzentrum für Schwerionenforschung, D-64291 Darmstadt, Germany

8 Present address: Institut de Physique Nucléaire, CNRS-IN2P3, 91406 Orsay, France

via three-body β^+-decay or via two-body electron-capture (EC) decay ($p + e^- \rightarrow n + \nu_e$). A measurement of the electron-capture decay constant of hydrogen-like $^{140}Pr^{58+}$ ions in the experimental storage ring (ESR) found this value to be increased by a factor of 1.49(8) compared to helium-like $^{140}Pr^{57+}$ [4]. This is counter-intuitive since one would expect the He-like charge state to decay more rapidly because the electron density at the nucleus is roughly twice as large as in H-like Pr [5]. This observation was explained by taking the conservation of total angular momentum into account [6–8]. However, this argument relies on a positive nuclear magnetic moment of ^{140}Pr, which has so far not been measured but is deduced from the magnetic moments of neighboring nuclei [4]. Similar enhancement has been measured in hydrogen-like $^{142}Pm^{60+}$ ions [9]. Suppression of the EC decay rate has been seen in hydrogen-like $^{122}I^{52+}$ ions as compared to the helium-like charge state [10]. In the latter case the quantum numbers of the involved states confirm the hypothesis formulated in [6–8].

The observation offers also interesting opportunities for laser spectroscopy at the ESR: EC from the upper hyperfine state in the hydrogen-like ion is hindered by angular momentum conservation, hence, laser excitation from the lower to the upper hyperfine state should result in a considerable increase of the nuclear lifetime in the storage ring. Moreover, optical pumping with circularly polarized light could be used to orient the nuclear spin parallel or antiparallel to the direction of movement. Due to the parity violating weak force, the neutrino emission can occur only in one direction after polarization.

This can be studied with the improved Schottky diagnosis system at the ESR. As demonstrated in Fig. 1 [11] the change in revolution frequency immediately following the EC decay can be used to detect the direction of the neutrino emission. The distribution of emission angles should change considerably after optical pumping with circularly polarized light.

A prerequisite for such experiments is the precise knowledge of the magnetic moment μ_I of the ^{140}Pr nucleus, which can be determined from the hyperfine splitting using collinear laser spectroscopy. If the magnetic moment has about the expected size, the transition wavelengh of the M1 hyperfine transition would be of the order of 1 μm and laser spectroscopy with resonance fluorescence detection would be possible as it has already been demonstrated at the ESR for cases with similar large splittings [12, 13]. Therefore, the magnetic moment of ^{140}Pr was proposed to be measured at ISOLDE/CERN by laser spectroscopy of the singly charged ion. The $4f^3 6s\ ^5I_4 \rightarrow 4f^3 6p\ ^5H_3$ transition from the ground state of the ion was identified to be suitable. First measurements of the corresponding hyperfine structure (hfs) in the stable isotope ^{141}Pr were performed at the TRIGA-LASER beamline [14, 15] at the Institute for Nuclear Chemistry in Mainz to serve as a reference for the on-line work. Results from both activities are presented.

2 Off-line spectroscopy of ^{141}Pr at TRIGA-LASER

2.1 TRIGA-LASER beamline

The ion beamline at the TRIGA research reactor is depicted in Fig. 2. It is supposed to receive ions either from the online connection to the TRIGA research reactor [14, 16, 17] with an energy of 30 keV (not shown in the figure) or from an offline ion source. The offline ion source, which was used for the Pr measurements consists of a resistively heated graphite tube which can surface ionize alkaline elements, earth-alkalines and some lanthanides. Extraction optics are used to shape the ion beam to a nearly collimated beam. The ion source is installed on a high-voltage platform that can be raised to about 20 kV against the beam line at ground potential. A 10° electrostatic deflector is used to superimpose the

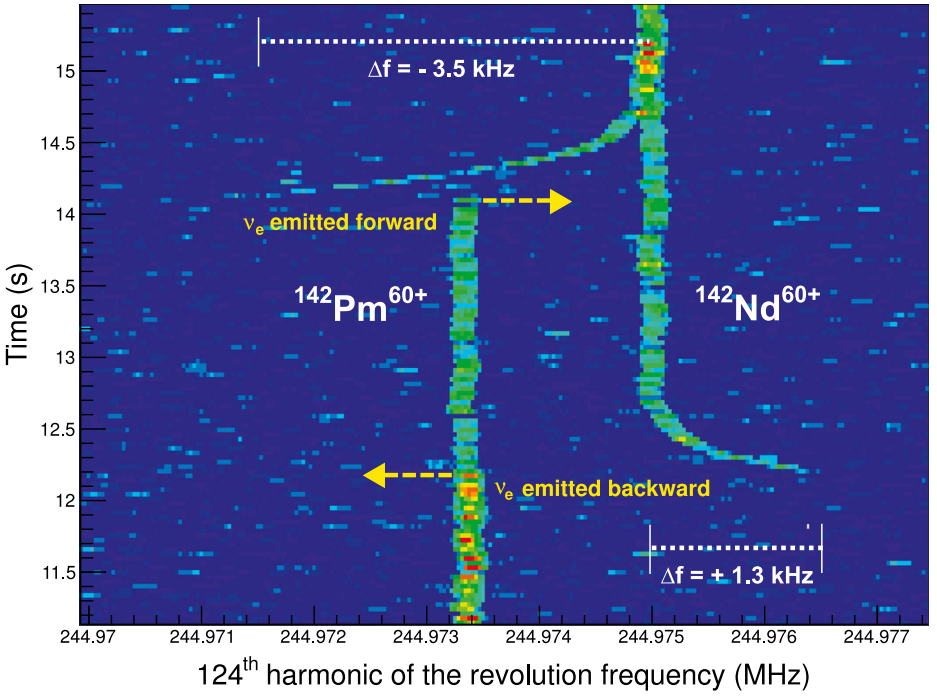

Fig. 1 Time excursion of the Schottky Spectrum of electron-cooled hydrogen-like $^{142}Pm^{60+}$ and fully-ionized $^{142}Nd^{60+}$ ions measured in the ESR. The time runs from bottom to top starting from injection of just two hydrogen-like $^{142}Pm^{60+}$ ions into the ESR. At about 12 s after injection, one from two ions decays through EC decay turning into $^{142}Nd^{60+}$ ion. The time of disappearance of the parent ion and the time of the appearance of the daughter ion are clearly seen and are correlated. The velocity of the daughter ion is modified due to the neutrino emission, which is seen by the offset in frequency. The electron cooler cools this velocity difference away, which is seen by the curved "cooling" tail. Since the optics of a storage ring averages away any transverse component of the recoil (stability condition of a ring inevitably requires particles to have phase advance), the seen frequency difference corresponds directly to the longitudinal component of the recoil and thus the direction of the neutrino emission can be deduced. The second EC decay occurs at around 14 s. Figure taken without changes from [11]

ion beam with the laser beam. Subsequently, an x-y deflector pair allows one to control the ion beam direction and a quadrupole doublet is used for further collimation. Adjustable apertures are located in the beamline in front and behind the fluorescence detection region (FDR) to optimize the overlap between the ion and the laser beam. The shape and intensity of the ion beam can be investigated using the beam diagnostics unit at the end of the beamline including a Faraday cup (FC) to measure the total beam current and a multichannel plate (MCP) combined with a fluorescent screen, on which the transversal shape of the ion beam can be observed with a camera. Laser beams are transported from the laser laboratory to the reactor hall via a pair of 180-m long single-mode fibers. Coupling into the beamline is achieved in either collinear or anticollinear geometry through viewports that are mounted at Brewster angle. Fluorescence spectra are recorded with the laser stabilized at a fixed frequency through Doppler-tuning the laser frequency in the rest frame of the ions using a variable voltage applied to the FDR. This scanning voltage is generated by amplifying the output of a ± 10 V 16-bit DAC card with a Kepco BOP500 voltage amplifier (amplification

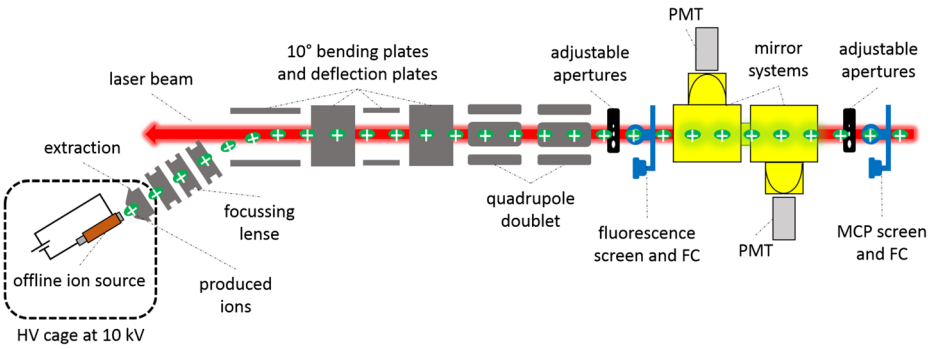

Fig. 2 Layout of the TRIGA-LASER beamline [14]. Ions are delivered from an off-line surface ion source mounted directly at the 10°-deflector. The laser is superimposed collinearly with the ion beam and resonance fluorescence is detected in two photomultiplier tubes (PMT). The beam diagnostics unit at the end of the beamline consists of a Faraday cup (FC) and a multichannel plate (MCP) combined with a fluorescent screen. For more details, see text

factor 50). An additional offset voltage of up to ± 10 kV can be applied with a Heinzinger PNChp10000 high-voltage power supply.

2.2 Laser system

The setup of the frequency-doubled master-oscillator power-amplifier (MOPA) system is depicted in Fig. 3a: a diode laser in Littrow design operated at 782 nm delivered about 30 mW of light that was subsequently amplified in a tapered amplifier (TA) to about 1.4 W. The laser light was mode-matched to the resonantor's fundamental mode of a Tekhnoscan FD-SF-07 frequency doubler. Even though the output beam of the TA has an elliptical beam profile, an aspheric lens for mode-matching into the frequency doubler was sufficient to achieve hundreds of milliwatts in the second harmonic. After beam shaping using two cylindrical lenses, the UV light was coupled into a single-mode fiber (Nufern S405HP) and a transmission of about 40% towards the collinear beamline in the reactor experimental hall was obtained.

The diode laser was stabilized to a HighFinesse WS7 wavelength meter. While the wavelength of the light is determined only with a relative precision of 10^{-7}, frequency excursions of the laser can be suppressed to a large extent. This was demonstrated by recording the lasers frequency stability with a Menlo Systems frequency comb FC1500. The result is shown in Fig. 3b as a histogram of the beat frequency between the diode laser and the nearest mode of the frequency comb, which was tuned to be 30 MHz off. The frequency was measured over about 15 minutes with each measurement averaged for 1 s. The distribution is well represented by a Gaussian profile with a full width at half maximum (FWHM) of 350 kHz. A negligible drift of 180 kHz was observed. Recording a spectrum of stable ^{141}Pr takes only a few minutes and laser drifts can therefore be neglected for the extraction of the hyperfine parameters.

2.3 Laser spectroscopy of $^{141}Pr^{+}$

A typical spectrum of the hyperfine multiplet of $^{141}Pr^{+}$ is depicted in Fig. 4. The ion beam current was about 400 pA and the laser beam attenuated to 900 μW. Fitting a multiple Voigt function to the hyperfine multiplet (green line) is performed by calculating the

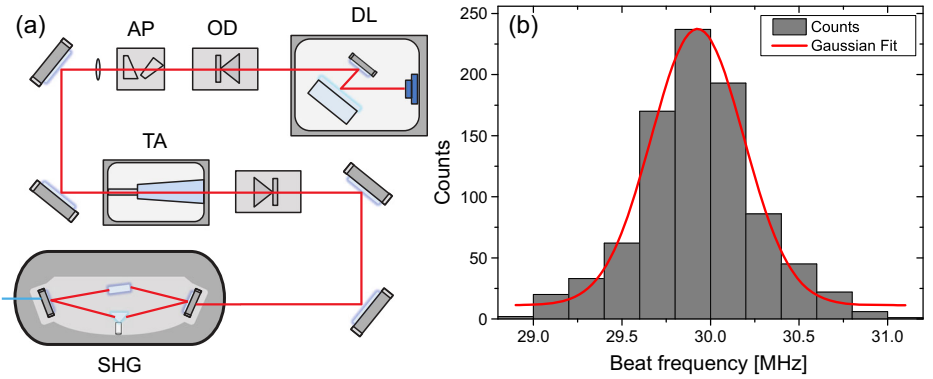

Fig. 3 **a** Setup of the master-oscillator power-amplifier (MOPA) system with a frequency doubler. The diode laser (DL) is protected against back reflections by an optical diode (OD). The elliptical output beam of the diode laser is transformed into a circular beam shape with an anamorphotic prism pair (AP). Two mirrors are used to couple the light into the tapered amplifier (TA). A second optical diode protects the TA against undesired back reflections. The amplified output beam is coupled into a second harmonic generator (SHG). **b** Frequency excursions of the extended-cavity diode laser built for the spectroscopy of Pr^+ at 793 nm measured with a frequency comb over a period of 15 min. Details see text

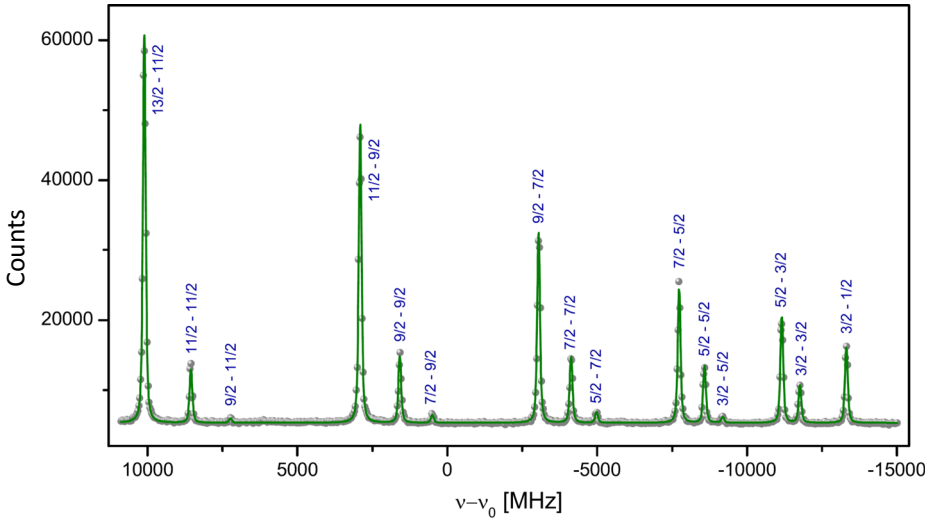

Fig. 4 The hyperfine multiplet of the investigated $4f^3 6s\ ^5I_4 \rightarrow 4f^3 6p\ ^5H_3$ transition in stable $^{141}Pr^+$ (grey). The change of the angular momentum J in the $J = 4 \rightarrow J' = 3$ transition and the nuclear spin $I(^{141}Pr) = 5/2$ results in a total of 15 hyperfine transitions, which are labelled with the respective F quantum numbers. They were fitted by a multiple Voigt profile (green) to extract A- and B-factors of the hyperfine structure (see Table 1). The frequency of the x-axis is given relative to the center of gravity of the hyperfine structure

relative positions of the individual peaks based on the A and B factors of the upper (u) and lower (l) states. Optimal parameters are determined by a χ^2-minimization varying $A_{l,u}$, $B_{l,u}$, intensities, linewidth parameters and baseline offset. The Voigt profil shows a FWHM of $w_L = 54(1)$ MHz for the Lorentzian part and $w_G = 95(1)$ MHz for the Gaussian contribution.

Table 1 Hyperfine structure parameter of the $4f^3 6s\ ^5I_4$ ground state and the $4f^3 6p\ ^5H_3$ excited state of $^{141}Pr^+$

$4f^3 6s\ ^5I_4$		$4f^3 6p\ ^5H_3$		
A_l (MHz)	B_l (MHz)	A_u (MHz)	B_u (MHz)	Reference
−239.7 (7)[1]	8.1 (53)	1030.0 (8)[3]	−29 (5)	this work
−231.8 (67)		891 (17)		[18]
		1031.6 (22)	12.2 (66)	[19]
		1030.9 (18)	14 (10)	[20]

Our result is listed with the statistical uncertainty in parantheses and the systematic uncertainty due to the uncertainty of the voltage amplification factor in brackets and compared to literature values

The extracted A and B factors of the upper and the lower states are listed in Table 1 and compared to literature values. The systematic uncertainty of 2.5×10^{-4} arises from the estimated uncertainties of the high voltages and the amplification factor of the Doppler-tuning voltage. Its contribution is negligible for the B factors. Our A factors agree with the two more recent literature values but have uncertainties improved by a factor of 10 and 2 in the ground and excited state, respectively. It should be noted that there is a misprint in [18], where an A-factor of −7.3 mK (= 219 MHz) is given for the ground state but using the hyperfine splitting of $W = -174$ (5) mK (5.22(15) GHz) provided in the same table, an A-factor of −7.73 (22) mK (= 231.8(67) MHz) is calculated in good agreement with our result. The A factor of the upper state in [18] is even more than 15% off but disagrees also with the other results reported in [19, 20]. The B-factor of the upper state is of opposite sign and clearly larger than those reported previously.

3 Spectroscopy of $^{135-137}$Pr at ISOLDE/CERN

3.1 Isotope production

Neutron-deficient Pr ($Z = 59$) isotopes were produced by spallation of Ta ($Z = 73$) combined with surface ionization of the Pr atoms at the general purpose mass separator (GPS) at ISOLDE. The measured production rate of ^{136}Pr was about 3.7×10^7 ions/μC (which corrsponds to about the same number of ions per second under standard production conditions during the beamtime). A direct measurement of the production rate of ^{140}Pr was unfortunately not possible since this isotope exhibits only a weak γ-line, but even with a rate two orders of magnitude smaller than that of ^{136}Pr, laser spectroscopy should still be feasible. However, the vast amount of radioactive isobars that cannot be separated by the mass separator led to an accumulation of radioactivity along the beamline that repeatedly caused alarms in the ISOLDE hall and proton beam intensity had to be reduced. Therefore, spectra of ^{140}Pr could not be recorded. Only the lighter isotopes ^{135,136,137}Pr were investigated.

3.2 Experimental setup

Detailed descriptions of the COLLAPS setup at ISOLDE are provided in [21–23]. Here, we will only briefly introduce details that are specific for the beamtime on Pr: A Coherent 899 titanium-sapphire laser was used to produce light at 781.2 nm. The laser was stabilized to a Fabry-Pérot interferometer which was again locked to a frequency-stabilized helium-neon (He:Ne) laser. A Bristol wavelength meter, calibrated with the stabilized He:Ne was used to

determine the laser wavelength. Frequency doubling was performed with a Spectra Physics Wavetrain and the UV beam ($\lambda^{-1} = 25600.808\ \mathrm{cm}^{-1}$) was superimposed with the 50-keV ion beam in the COLLAPS beamline. Due to the large size of the hyperfine structure, the Kepco BOP500 voltage amplifier that is usually used at COLLAPS for Doppler tuning similar to TRIGA-LASER (see Section 2.1), was replaced by a model BOP1000, which covers a tuning range of ±1000 V. To determine the amplification factor, a voltage ramp was regularly applied to the detection region and the applied voltage recorded with a high-voltage divider (Kepco scan). While the scans looked linear at first sight, closer inspection in the off-line analysis revealed a nonlinearity much larger than ever observed with the BOP500 model. This nonlinearity changed considerably with time, which strongly limited all trials to correct for it in the analysis. We could, nevertheless, extract the magnetic hyperfine splitting factor A with uncertainty at a level of a few percent. The systematic uncertainty caused by the nonlinearity was estimated by analyzing a spectrum of the stable isotope in connection with measurements of the Kepco amplifier output voltage over the same scanning range. It should be noted, however, that the systematic uncertainty is not correlated between the different isotopes as it is usually the case in collinear laser spectroscopy for the calibration uncertainty of absolute voltages.

3.3 Results

^{135}Pr: According to the known nuclear spin of $I = 3/2$ [24], we expect nine hyperfine lines in the $J = 4 \rightarrow J' = 3$ fine structure transition. During the beamtime two spectra were recorded, one of them shown in the top left of Fig. 5, exhibiting the four strongest transitions. The five missing resonances are expected to appear between the four strongest components with the strongest of them at an intensity of about 7% of the $F = 11/2 \rightarrow F' = 9/2$ transition.

^{136}Pr: With a nuclear spin of $I = 2$ [24], twelve hyperfine lines are expected. Again, only the 4 strongest resonances were observed and only a single spectrum that could be analyzed was recorded. It is shown on the top right in Fig. 5. The weakest observed line is enlarged in the inset. The missing components have much smaller intensities and are not expected to be observable at this noise level.

^{137}Pr: This isotope has the same nuclear spin as the stable isotope ^{141}Pr [24] and 15 hyperfine lines are expected similar to the spectrum shown in Fig. 4. Here, the ten most prominent lines were observed but the complete hyperfine structure could not be recorded in a single scan. Instead, it was distributed across three scan regions as depicted in the lower part of Fig. 5.

^{141}Pr: The stable isotope was also measured at ISOLDE using a reservoir for a stable isotope (mass marker) at ISOLDE. However, the strong nonlinearity of the amplifier caused very large uncertainties for all hyperfine parameters since the resonances were distributed across a large voltage range similar as in the case of ^{137}Pr. Therefore it is not at all competitive with the investigations performed at TRIGA-LASER.

The TRIGA-LASER measurements of ^{141}Pr were used as a reference to extract the nuclear magnetic moments of the three unstable isotopes, according to

$$\mu = \mu_{\mathrm{ref}} \frac{A \cdot I}{A_{\mathrm{ref}} \cdot I_{\mathrm{ref}}} \tag{1}$$

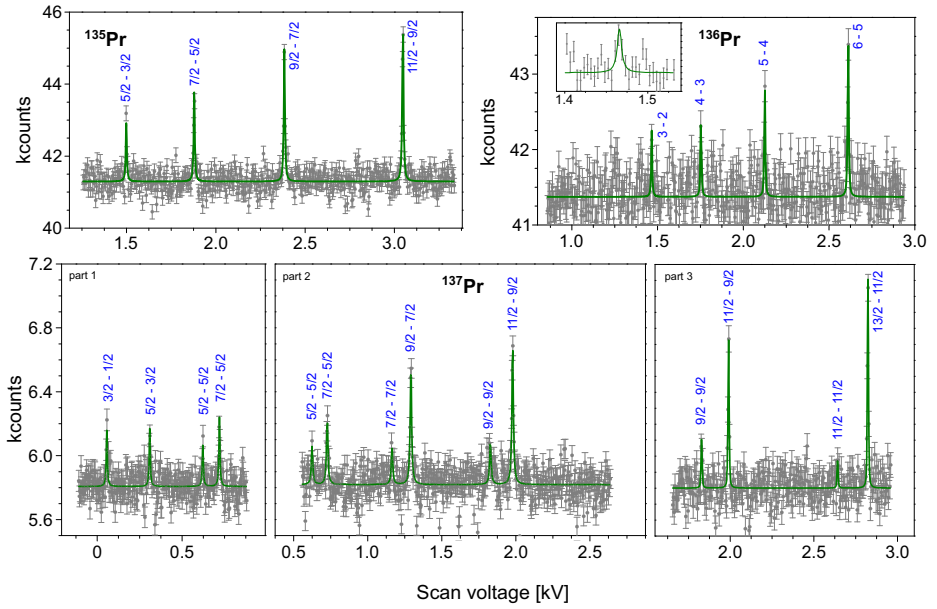

Fig. 5 Hyperfine structure in the $4f^3 6s\,{}^5\mathrm{I}_4 \rightarrow 4f^3 6p\,{}^5\mathrm{H}_3$ transition of ^{135,136,137}Pr as a function of the Doppler-tuning voltage. Only the strongest components of the 9, 12, and 15 expected hyperfine resonances for the isotopes with nuclear spin of $I = 3/2$, 2, and 5/2, respectively, are observed. For details see text

Table 2 Magnetic moments of the short-lived Pr isotopes studied at ISOLDE

Isotope	I	$\mu_I\,(\mu_\mathrm{N})$
^{135}Pr	3/2	2.00 (1)[12]
^{136}Pr	2	1.76 (1)[11]
^{137}Pr	5/2	3.67 (6)[22]

The nuclear spins are taken from Ref. [24]. Numbers in parentheses are the statistical uncertainties while those in brackets reflect the systematic uncertainty caused by the nonlinearity of the amplifier (see text)

with $\mu_\mathrm{ref} = 4.2754\,(5)\,\mu_\mathrm{N}$ [25] and our value $A_\mathrm{ref} = -239.7\,(7)[1]$ MHz from Table 1. The results are listed in Table 2 and have uncertainties that are by far dominated by the systematic uncertainty of the Doppler-tuning voltage caused by the nonlinearity of the Kepco amplifier (given in brackets). Hence, accuracy is limited on a level of approximately 6%, which is unusual for collinear laser spectroscopy. However, these are the only magnetic moments available for those isotopes so far.

4 Conclusion

We have performed collinear laser spectroscopy of the stable isotope ^{141}Pr$^+$ at the TRIGA-LASER setup in Mainz and of $^{135-137}$Pr$^+$ at ISOLDE/CERN. The magnetic moments of the neutron-deficient isotopes were determined for the first time but are afflicted with a rather large uncertainty due to a nonlinearity of the voltage amplifier applied for Doppler-tuning,

limiting the uncertainty to about 6%. The nuclear magnetic moment of the neutron-deficient isotope ^{140}Pr remains to be measured. It is required to facilitate laser spectroscopy on the hydrogen-like ion $^{140}Pr^{58+}$ in the ESR storage ring at GSI. Additionally, the explanation of the observed enhanced EC rates in hydrogen-like $^{140}Pr^{58+}$ as well as $^{142}Pm^{60+}$ ions and suppressed rate in $^{122}I^{52+}$ relies on the calculated magnetic moments. Here, the understanding of mechanisms of the decays of hydrogen-like ions may be important for modelling of stellar nucleosynthesis, in which the involved nuclei can be highly ionized [26, 27]. Furthermore, the results obtained for hydrogen-like ions affect the predicted decay characteristics of lithium-like ions [28].

Acknowledgements This work was supported by the Helmholtz Association (VH-NG148), the German Ministry for Science and Education (BMBF, 06MZ9178I), the Max-Planck-Society, the European Union Seventh Framework (Contract No. 262010) and the BriX IAP Research Program No. P6/23 (Belgium). A. K. acknowledges support from the Carl-Zeiss-Stiftung (AZ:21-0563-2.8/197/1), N.F. acknowledges support from the German Research Foundation under Grant DFG/GRK 1581 (Symmetry Breaking).

References

1. Folan, L.M., Tsifrinovich, V.I.: Phys. Rev. Lett. **74**, 499 (1995)
2. Litvinov, Y.A., Bosch, F.: Rep. Prog. Phys. **74**, 6301 (2011)
3. Nica, N.: Nucl. Data Sheets **108**(7), 1287 (2007)
4. Litvinov, Y.A., Bosch, F., Geissel, H., Kurcewicz, J., Patyk, Z., Winckler, N., Batist, L., Beckert, K., Boutin, D., Brandau, C., Chen, L., Dimopoulou, C., Fabian, B., Faestermann, T., Fragner, A., Grigorenko, L., Haettner, E., Hess, S., Kienle, P., Knöbel, R., Kozhuharov, C., Litvinov, S.A., Maier, L., Mazzocco, M., Montes, F., Münzenberg, G., Musumarra, A., Nociforo, C., Nolden, F., Pfützner, M., Plaß, W.R., Prochazka, A., Reda, R., Reuschl, R., Scheidenberger, C., Steck, M., Stöhlker, T., Torilov, S., Trassinelli, M., Sun, B., Weick, H., Winkler, M.: Phys. Rev. Lett. **99**, 262501 (2007)
5. Bambynek, W., Behrens, H., Chen, M.H., Crasemann, B., Fitzpatrick, M.L., Ledingham, K.W.D., Genz, H., Mutterer, M., Intemann, R.L.: Rev. Mod. Phys. **49**, 77 (1977)
6. Patyk, Z., Kurcewicz, J., Bosch, F., Geissel, H., Litvinov, Y.A., Pfützner, M.: Phys. Rev. C **77**, 14306 (2008)
7. Ivanov, A.N., Faber, M., Reda, R., Kienle, P.: Phys. R. C **78**, 25503 (2008)
8. Siegień-Iwaniuk, K., Winckler, N., Bosch, F., Geissel, H., Litvinov, Y.A., Patyk, Z.: Physi. Rev. C **84**, 14301 (2011)
9. Winckler, N., Geissel, H., Litvinov, Y., Beckert, K., Bosch, F., Boutin, D., Brandau, C., Chen, L., Dimopoulou, C., Essel, H., Fabian, B., Faestermann, T., Fragner, A., Haettner, E., Hess, S., Kienle, P., Knöbel, R., Kozhuharov, C., Litvinov, S., Mazzocco, M., Montes, F., Münzenberg, G., Nociforo, C., Nolden, F., Patyk, Z., Plaß, W., Prochazka, A., Reda, R., Reuschl, R., Scheidenberger, C., Steck, M., Stöhlker, T., Torilov, S., Trassinelli, M., Sun, B., Weick, H., Winkler, M.: Phys. Lett. B **679**(1), 36 (2009)
10. Atanasov, D.R., Winckler, N., Balabanski, D., Batist, L., Bosch, F., Boutin, D., Brandau, C., Dimopoulou, C., Essel, H.G., Faestermann, T., Geissel, H., Hachiuma, I., Hess, S., Izumikawa, T., Kienle, P., Knöbel, R., Kozhuharov, C., Kurcewicz, J., Kuzminchuk, N., Litvinov, S.A., Litvinov, Y.A., Mao, R.S., Märtin, R., Mazzocco, M., Münzenberg, G., Namihira, K., Nolden, F., Ohtsubo, T., Patyk, Z., Reuschl, R., Sanjari, M.S., Scheidenberger, C., Shubina, D., Spillmann, U., Steck, M., Stöhlker, T., Sun, B., Suzuki, T., Trassinelli, M., Tupitsyn, I.I., Weick, H., Winkler, M., Winters, D.F.A., Yamaguchi, T.: Eur. Phys. J. A **48**, 22 (2012)
11. Kienle, P., Bosch, F., Bühler, P., Faestermann, T., Litvinov, Y., Winckler, N., Sanjari, M., Shubina, D., Atanasov, D., Geissel, H., Ivanova, V., Yan, X., Boutin, D., Brandau, C., Dillmann, I., Dimopoulou, C., Hess, R., Hillebrand, P.M., Izumikawa, T., Knöbel, R., Kurcewicz, J., Kuzminchuk, N., Lestinsky, M., Litvinov, S., Ma, X., Maier, L., Mazzocco, M., Mukha, I., Nociforo, C., Nolden, F., Scheidenberger, C., Spillmann, U., Steck, M., Stöhlker, T., Sun, B., Suzaki, F., Suzuki, T., Torilov, S., Trassinelli, M., Tu, X., Wang, M., Weick, H., Winters, D., Winters, N., Woods, P., Yamaguchi, T., Zhang, G., Ohtsubo, T.: Phys. Lett. B **726**(4), 638 (2013)
12. Seelig, P., Borneis, S., Dax, A., Engel, T., Faber, S., Gerlach, M., Holbrow, C., Huber, G., Kühl, T., Marx, D., Meier, K., Merz, P., Quint, W., Schmitt, F., Tomaselli, M., Völker, L., Winter, H., Würtz, M.,

Beckert, K., Franzke, B., Nolden, F., Reich, H., Steck, M., Winkler, T.: Phys. Rev. Lett. **81**(22), 4824 (1998)
13. Ullmann, J., Andelkovic, Z., Brandau, C., Dax, A., Geithner, W., Geppert, C., Gorges, C., Hammen, M., Hannen, V., Kaufmann, S., König, K., Litvinov, Y., Lochmann, M., Maas, B., Meisner, J., Murböck, T., Sánchez, R., Schmidt, M., Schmidt, S., Steck, M., Stöhlker, T., Thompson, R., Trageser, C., Vollbrecht, J., Weinheimer, C., Nörtershäuser, W.: Nat. Commun. **8**, 15484 (2017)
14. Ketelaer, J., Krämer, J., Beck, D., Blaum, K., Block, M., Eberhardt, K., Eitel, G., Ferrer, R., Geppert, C., George, S., Herfurth, F., Ketter, J., Nagy, S., Neidherr, D., Neugart, R., Nörtershäuser, W., Repp, J., Smorra, C., Trautmann, N., Weber, C.: Nucl. Instrum. Methods Phys. Res., Sect. A, pp. 162 (2008)
15. Gorges, C., Blaum, K., Frömmgen, N., Geppert, C., Hammen, M., Kaufmann, S., Krämer, J., Krieger, A., Neugart, R., Sánchez, R., Nörtershäuser, W.: J. Phys. B: At., Mol. Opt. Phys. **48**(24), 245008 (2015)
16. Eibach, M., Beyer, T., Blaum, K., Block, M., Eberhardt, K., Herfurth, F., Geppert, C., Ketelaer, J., Ketter, J., Krämer, J., Krieger, A., Knuth, K., Nagy, S., Nörtershäuser, W., Smorra, C.: Nucl. Instrum. Methods Phys. Res., Sect. A **613**(2), 226 (2010)
17. Beyer, T., Blaum, K., Block, M., Düllmann, C.E., Eberhardt, K., Eibach, M., Frömmgen, N., Geppert, C., Gorges, C., Grund, J., Hammen, M., Kaufmann, S., Krieger, A., Nagy, S., Nörterhäuser, W., Renisch, D., Smorra, C., Will, E.: Appl. Phys. B **114**(1), 129 (2014)
18. Ginibre, A.: Phys. Scr. **39**(6), 694 (1989)
19. Maosheng, L., Hongliang, M., Miaohua, C., Fuquan, L., Jiayong, T., Fujia, Y.: Phys. Rev. A **62**, 052504 (2000)
20. Furmann, B., Stefańska, D., Stachowska, E., Ruczkowski, J., Dembczyński, J.: Eur. Phys. J. D **17**(3), 275 (2001)
21. Mueller, A., Buchinger, F., Klempt, W., Otten, E., Neugart, R., Ekström, C., Heinemeier, J.: Nucl. Phys. A **403**, 234 (1983)
22. Neugart, R., Billowes, J., Bissell, M.L., Blaum, K., Cheal, B., Flanagan, K.T., Neyens, G., Nörtershäuser, W., Yordanov, D.T.: J. Phys. G **44**(6), 064002 (2017)
23. Krieger, A., Nörtershäuser, W., Geppert, C., Blaum, K., Bissell, M.L., Frömmgen, N., Hammen, M., Kreim, K., Kowalska, M., Krämer, J., Neugart, R., Neyens, G., Sánchez, R., Tiedemann, D., Yordanov, D.T., Zakova, M.: Appl. Phys. B **123**(1), 15 (2017)
24. Firestone, R.B., Shirley, V.S.: Table of Isotopes, 8th edn. Wiley, New York (1998)
25. Stone, N.: At. Data Nucl. Data Tables **90**(1), 75 (2005)
26. Takahashi, K., Yokoi, K.: At. Data Nucl. Data Tables **36**, 375 (1987)
27. Bosch, F., Litvinov, Y.A., Stöhlker, T.: Prog. Part. Nucl. Phys. **73**, 84 (2013)
28. Siegień-Iwaniuk, K., Patyk, Z.: Phys. Rev. C **84**, 64309 (2011)